This paper describes objective technical results and analysis. Any subjective views or opinions that might be expressed in the paper do not necessarily represent the views of the U.S. Department of Energy or the United States Government.

ASME 2019 Pressure Vessels & Piping Conference
SAND2019-8524C
July 14-19, 2019, San Antonio, Texas, USA

PVP2019-93755

Analysis of EDSVessel Clamping system and door seal

Jerome H Stofleth
Sandia National Laboratories
Albuquerque, NM, USA

Megan K Tribble
Sandia National Laboratories
Albuquerque, New Mexico, USA

John Ludwigsen
Sandia National Laboratories
Albuquerque, New Mexico, USA

Robert W Crocker
Sandia National Laboratories
Livermore, CA, USA

ABSTRACT

The V26 containment vessel was procured by the Project Manager, Non-Stockpile Chemical Materiel (PMNSCM) for use on the Phase-2 Explosive Destruction Systems. The vessel was fabricated under Code Case 2564 of the ASME Boiler and Pressure Vessel Code, which provides rules for the design of impulsively loaded vessels. The explosive rating for the vessel, based on the Code Case, is nine (9) pounds TNT-equivalent for up to 637 detonations, limited only by fatigue crack growth calculations initiated from a minimum detectable crack depth.

The vessel consists of a cylindrical cup, a flat cover or door, and clamps to secure the door. The vessel is sealed with a metal gasket. The body is a deep cylindrical cup machined from a 316 stainless steel forging. The door is also machined from a 316 stainless steel forging. The closure clamps are secured with four 17-4 PH steel threaded rods with 4140 alloy steel threaded-nuts on one end and hydraulic nuts on the other.

A flange with four high-voltage electrical feedthroughs is bolted to the door and sealed with a small metal gasket. These feedthroughs conduct the firing signals for the high-voltage Exploding Bridge-wire detonators. Small blast plates on the inside of the door protect fluidic components and electrical feedthroughs. A large blast plate provides additional protection.

Both vessel door and feedthrough flange employ O-ring seals outside the metal seals in order to provide a mechanism for helium leak checks of the volume just outside the metal seal surface before and after detonation.

In previous papers (References 2 and 3), the authors describe results from testing of the vessel body and ends under qualification loads, determining the effective TNT equivalency of Composition C4 (EDS Containment Vessel TNT Equivalence Testing) and analyzing the effects of distributed explosive charges versus unitary charges (EDS Containment Vessel Explosive Test and Analysis).

In addition to measurements made on the vessel body and ends as reported previously, bulk motion and deformation of the door and clamping system was made. Strain gauges were positioned at various locations on the inner and outer surface of the clamping system and on the vessel door surface. Digital Image Correlation was employed during both hydrostatic testing and dynamic testing under full-load explosive detonation to determine bulk and bending motion of the door relative to the vessel body and clamping system. Some limited hydrocode and finite element code analysis was performed on the clamping system for comparison.

The purpose of this analysis was to determine the likelihood of a change in the static sealing efficacy of the metal clamping system and to evaluate the possibility of dynamic burping of vessel contents during detonation. Those results will be reported in this paper.

INTRODUCTION

The Explosive Destruction System (EDS), which was developed at Sandia National Laboratories, is used by the US Army to destroy recovered chemical munitions. The apparatus treats chemical munitions through explosive access using shaped charges, followed by chemical neutralization of the agents. The process is conducted inside a stainless steel vessel which fully contains the detonation and serves as a chemical reactor.

Vessels are fabricated per Section VIII Division 3 of the ASME Boiler and Pressure Vessel Code and Code Case 2564. The Vessel Design Specification required by the ASME Code Case specifies a quantity and location of explosives to be used

jhstofl@sandia.gov
Copyright © 2019 by ASME

Sandia National Laboratories is a multimission laboratory managed and operated by National Technology & Engineering Solutions of Sandia, LLC, a wholly owned subsidiary of Honeywell International Inc., for the U.S. Department of Energy's National Nuclear Security Administration under contract DE-NA0003525.

as the design basis impulse for the vessel [1]. The original vessel was designed and tested for a maximum explosive loading from a centrally-located charge. To provide the maximum flexibility to treat a variety of recovered munitions in the EDS, newer vessels are designed and tested for the maximum explosive loading from a distributed 6-charge configuration that mimics the munitions geometry that represents a maximum credible load on the system.

Dynamic experiments, hydrostatic testing and hydrocode and finite element analyses have been performed previously on this vessel type for several configurations and charge loads. Qualification tests were also conducted in both the unitary geometry and the distributed geometry. Currently, this vessel type is qualified for a 7.2lbs TNT equivalent unitary charge, and a 9lbs TNT equivalent distributed 6-charge geometry.

In previous papers, the authors describe results from testing of the vessel body, ends and door under qualification loads, determining the effective TNT equivalency of Composition C4 [2] and analyzing the effects of distributed explosive charges versus unitary charges [3]. The results of these analyses showed that, for the distributed charge configuration, there is a decrease in dynamic cylindrical body deformation of the vessel but an increase in dynamic loading on the vessel aft end, door, and door clamping system as compared to the unitary charge configuration. Further, future charge configurations may include a closer proximity of these distributed charges to the door and aft end. Therefore, an understanding of the dynamics of the door and seal during detonation is imperative to the continued success of the system.

In addition to measurements made on the vessel body and aft end as reported previously, bulk motion and deformation of the door and door clamping system was made during these tests through the use of strain gages and Digital Image Correlation (DIC) analysis. Strain gauges were positioned at various locations on the inner and outer surface of the clamping system and on the vessel door surface. Digital Image Correlation was employed during both hydrostatic testing and dynamic testing to determine bulk and bending motion of the door relative to the vessel body and clamping system and any potential loss of door seal integrity.

The purpose of this report is to demonstrate the effectiveness of the vessel/door seal during dynamic qualification of the system, and to measure any change in the static sealing efficacy of the metal seal. The effect of dynamic "burping" of vessel during detonation will also be reviewed. These results will be reported in this paper.

VESSEL

The vessel consists of a cylindrical cup, a flat cover or door, and clamps to secure the door. The vessel is sealed with a metal gasket. The body is a deep cylindrical cup machined from a 316 stainless steel forging. The door is also machined from a 316 stainless steel forging. The closure clamps are machined from 4140 alloy steel and are secured with four 17-4 PH steel threaded rods with 4140 alloy steel threaded-nuts on one end and hydraulic nuts on the other. The vessel door employs a flange mounted on its surface for access to high voltage feedthroughs used to transmit electrical signals to the detonators. There are several additional penetrations through the vessel door to allow for liquid and gaseous sampling of the vessel content during chemical neutralization of the munitions contents. The high voltage flange relies on a similar metal seal to maintain the integrity of the high voltage flange. The seal rings are made from 17-4 PH steel. Pertinent vessel dimensions are provided below in Table 1.

Table 1: Dimensional properties for vessel components.

Overall length	71.89 inches
Inside length	56.58 inches
Outside diameter	36.53 inches
Inside diameter	29.22 inches
Door thickness	9.00 inches
Cylinder wall thickness	3.65 inches
Aft end thickness	6.30 inches

This EDS vessel is designed with a vessel body and door flange that is engaged by a two-piece perimeter clamping system which is tightened via 4 three-inch threaded rods oriented laterally to the vessel axis. Figure 1 shows a photograph of the vessel body with seal ring mounted.

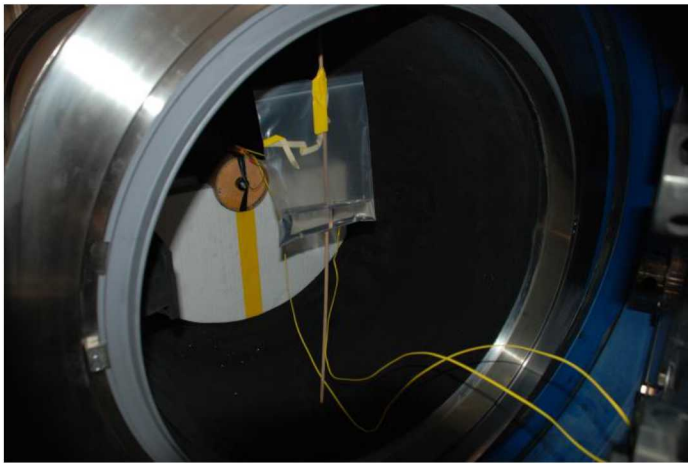

Figure 1: EDS vessel with seal ring mount on body.

The vessel body surface is manufactured with a beveled inner surface that is designed to engage a metal seal ring in order to enable a hermetic seal of the vessel volume. There is a secondary O-ring mounted to the door outside the metal seal ring, which allows a volume to be created between them for helium leak check purposes only. This O-ring is not designed to act as a vessel seal during dynamic use. The door employs a matching beveled surface which contacts the opposite side of the seal ring. When the clamps are engaged via hydraulic nuts, the beveled surfaces of the seal ring are pulled into the matching beveled surfaces on the vessel body and door, flexing the seal ring wings and engaging a hermetic seal (see Figure 2). The clamp and rod geometry are shown in Figures 3 and 4.

Copyright © 2019 by ASME

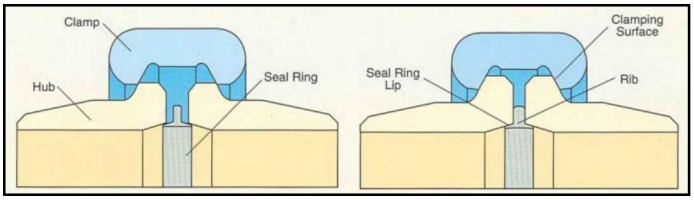

Figure 2: EDS vessel with seal ring mount on body.

STRAIN MEASUREMENT

Dynamic strain gauges (Vishay EP-08-250BG-120, 120 ohm, biaxial) were installed on the EDS vessel at several locations. In addition, plastic strain, or permanent vessel deformation, was measured after each test at six locations along the length of the vessel by measuring the outer diameter using a stainless steel π-tape around the circumference and validated through post-test signal processing techniques as reported previously. Gage locations and orientations are tabulated in Table 2 and shown in Figures 3 and 4.

Table 2: Strain gage location and orientation.

Gauge	Hoop/Axial	Location
1	H	Aft center
1	A	Aft center
2	H	Vessel body 1/3 from aft
3	A	Vessel body 2/3 from aft
4	H	Vessel body mid-point
5	H	Clamp outside
5	A	Clamp outside
6	H	Clamp inside
6	A	Clamp inside
7	H	Door center

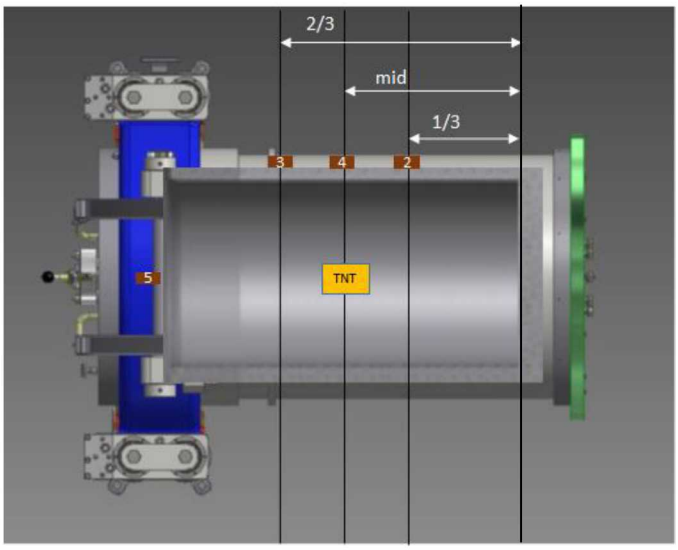

Figure 3: EDS vessel – side/interior view. Gages 2,3,4 shown on body, gage 5 shown on exterior clamp.

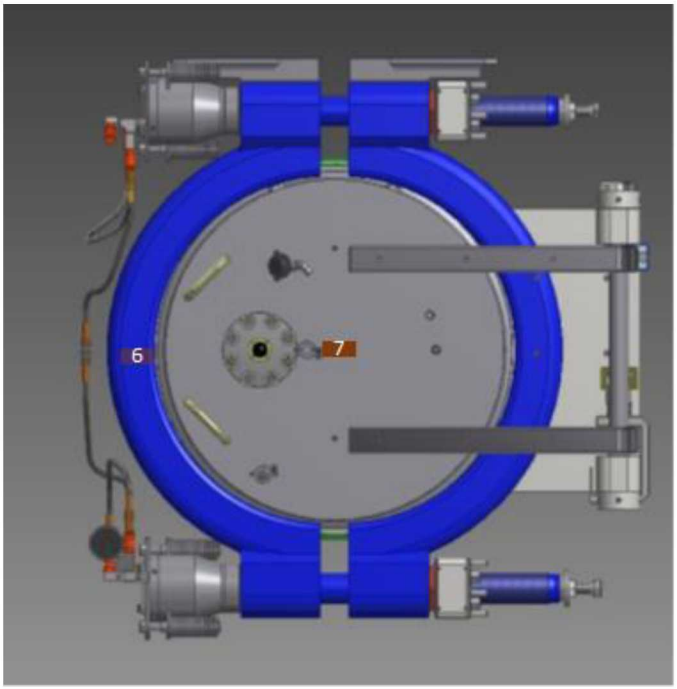

Figure 4: EDS vessel – door/clamp view. Gage 7 shown on door-center, gage 6 shown at interior clamp. Gage 1 is opposite (aft) end, center.

DIGITAL IMAGE CORRELATION

Digital Image Correlation is a method which employs two cameras separated by a predetermined distance to produce a stereo view of an object surface. Knowing the baseline separation of the cameras, their orientation to the object surface, and the distance to the object from the camera(s) baseline, one can use a classic photogrammetry algorithm to produce out-of-plane motion of the object surface at the frame-rate of the cameras.

Many steps are required in the setup for producing a frame of reference for the cameras and object plane, calibration of the imaging system, and application of the object fiducial – these steps will not be described here but can be found in the literature for DIC imaging [4]. As well, many parameters play into the spatial and temporal resolution and error in the measurements made with this system.

For these particular tests, the temporal resolution (frame-rate of cameras) was set at twenty five thousand frames per second (40 microseconds per image pair), with an inter-frame jitter of one percent of the frame rate. The two cameras were connected so as to maintain synchronization between like frames from each camera. The spatial resolution was determined to be approximately 2 millimeters per pixel, with a spatial error of +/-0.03mm at 1σ, or +/-0.06mm at 3σ in the out-of-plane dimension [5]. In general however, any camera system may be used. The implementation of this system was performed by the Sandia National Laboratories, Photometrics Department.

The cameras are set up on a baseline that is parallel to the proposed image plane, and centered about an axis that is perpendicular to the object plane through the centroid of the

Copyright © 2019 by ASME

object. The object to be imaged is painted with a pseudo-random speckle pattern so that an image correlation algorithm can track each dot in the pattern as its apparent baseline is offset in the vertical and/or horizontal images between the synchronized frames of each camera. The algorithm then resolves this apparent planer offset motion as out-of-plane displacement perpendicular to the image plane. Commercial software [6] then produces a time determined, pixel by pixel, three-dimensional surface displace of the object.

This data may then be rendered as a point-tracking, a line "cut" tracking or an entire surface deformation representation. The image in Figure 5 show a front-view of the EDS vessel door with the speckle pattern painted on the surface and the displacement data overlay through a view from one of the imaging cameras.

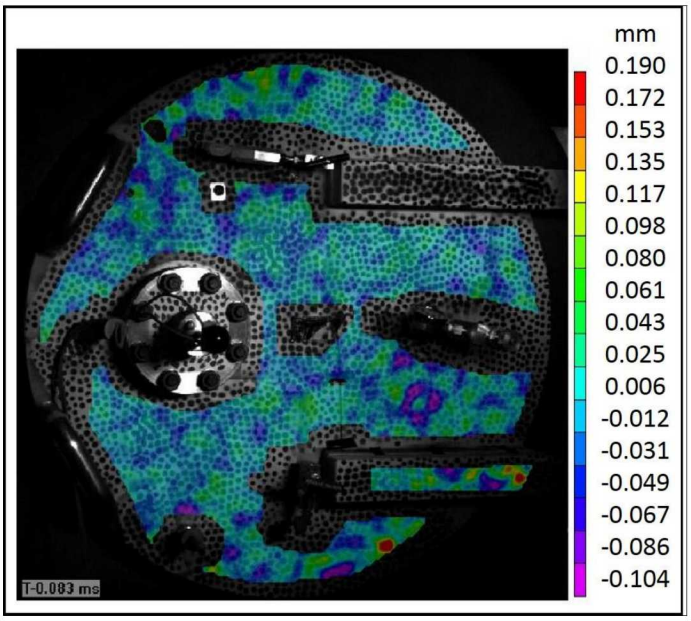

Figure 5: Door/clamp view with speckle pattern.

HYDROTEST RESULTS

The hydrotest was conducted from zero pressure up to 2,850 psi, the ASME static pressure rating of the EDS vessel. Displacements were measured at seven locations around the door; three points around the door edge, one point on each of the two door arms, and two points near the center of the door, as denoted in Figure 6 as highlighted rectangles. The distance between the clamps and the gap between the vessel and the door was also measured during the hydrotest as shown in Table 3.

Figure 6 shows data from DIC during the hydrotest at pressures from zero to 1700 psi, where the color scale indicates the out-of-plane displacement at each point measured in millimeters. Note that the scales for each sub-image vary in an attempt to maintain a reasonable image-color dynamic range.

Some of these data, along with feeler gage measurements between the vessel and door, are plotted in Figures 7 and 8 and tabulated in Table 3. After 1700 psi, one of the DIC camera was disturbed causing a loss of calibration. The system was recalibrated at 2000 psi, and additional displacements at higher pressure were measured relative to this new baseline. The displacement between 1700 and 2000 psi is unknown, so absolute displacement can be not be determined above 1700 psi. Figure 9 shows the change in displacement between 2000 psi and 2850 psi.

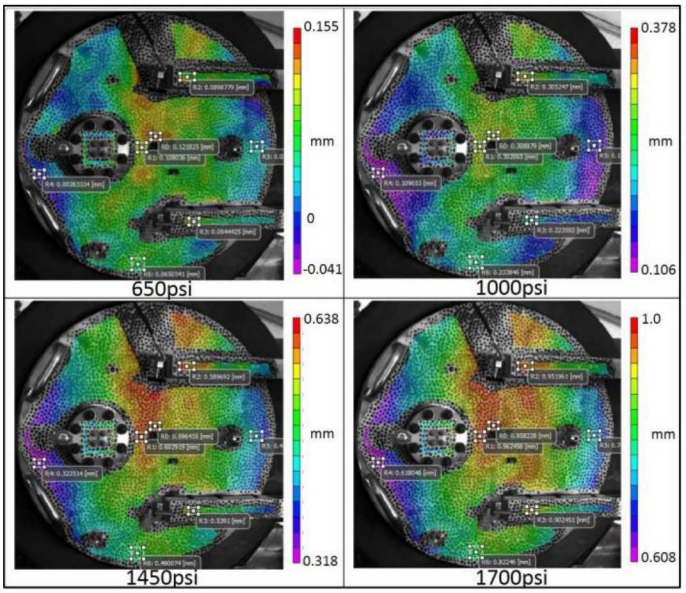

Figure 6: DIC displacement measurement overlaid on vessel door at various hydrostatic pressures.

Table 3: Door displacement date from hydrotest in millimeters.

Pressure (psi)	Feeler gage	DIC center	DIC bottom	DIC left side	DIC right side
0	0	0	0	0	0
650	0.102	0.104	0.067	-0.022	0.025
1000	0.203	0.291	0.236	0.085	0.170
1450	0.254	0.578	0.492	0.298	0.430
1700	0.356	0.940	0.824	0.593	0.750
2000	0.269				
2500	0.610				
2850	0.965				
0	0.058				

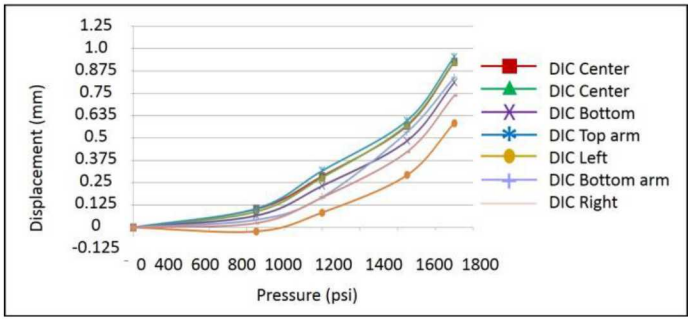

Figure 7: Door displacement data from hydrotest.

Comparison of the DIC measurements at the center and edges of the door indicates that there was more translation than bending of the door – the minimum displacement near the edge

Copyright © 2019 by ASME

was 0.584mm, while the difference between the largest displacement at the door center and smallest near the edge was 0.356mm. DIC shows considerably greater movement than do the feeler gages, i.e. the door moved without opening a proportionately sized gap between the clamping flanges on the vessel and the door. Assuming both measurement methods were accurate, this suggests that much of the movement of the door resulted from bending of the clamping flanges at about 1000psi, which is not measured by the feeler gages.

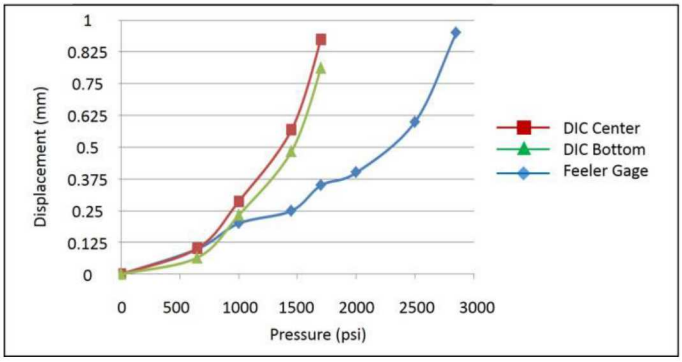

Figure 8: Comparison of DIC and feeler gage measurements.

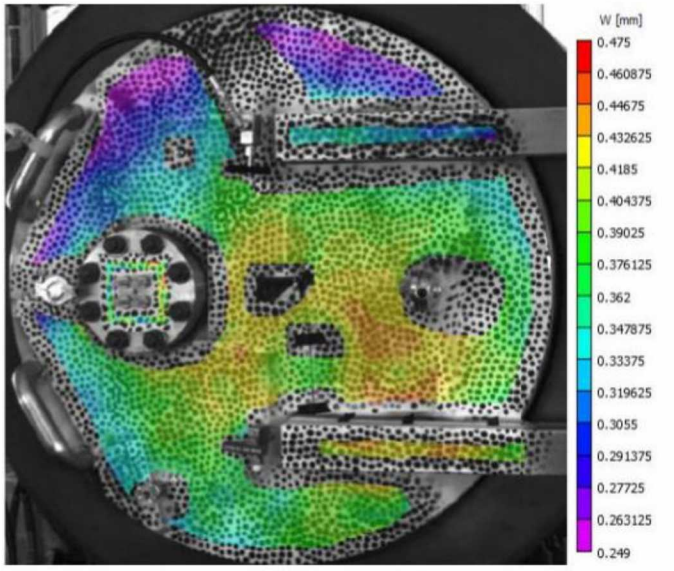

Figure 9: Displacement at 2850psi relative to 2000psi.

Figure 10 shows the gap between the two clamps during the hydrotest. Initially, the gap on the bottom got smaller as the top got bigger, which appears more like a repositioning of the clamps than strain. Thereafter, both gaps increased slightly. The total combined increase was 1.5 millimeters at 1700 psi and 2 millimeters at 2850 psi. The transfer function between elongation of the threaded rods and movement of the door is complex, particularly if deformation of the flange causes the contact angle between the clamp and the flange to change.

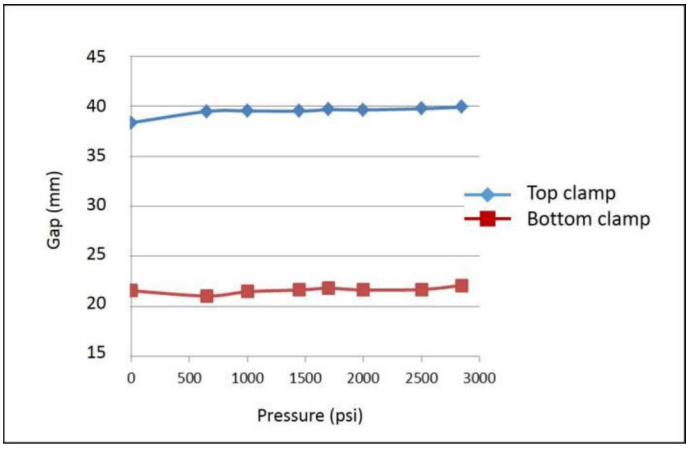

Figure 10: Gap between clamps during hydrotest.

DYNAMIC TEST RESULTS

The dynamic test consisted of a distributed charge of 9lbs of Composition C-4 (11.25lbs TNT equivalent), which represents a 125% dynamic over-test for this vessel as required per Code Case 2564. The charges were detonated simultaneously using Exploding Bridge-wire (EBW) detonators, which have a quoted jitter of 200ns. Details of the charge type and geometry are shown in Figure 11 and results of the tests can be found in reference 3.

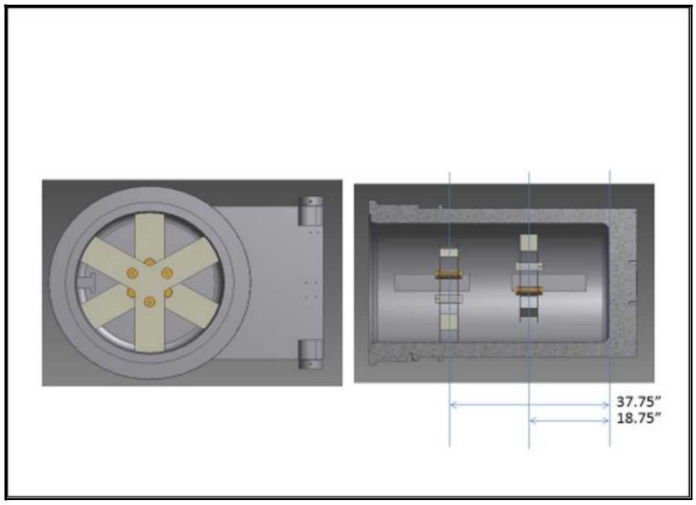

Figure 11: Basic layout of qualification load charges.

Figure 12 shows the strain data from the dynamic test from gage 7 (Table 2) mounted near the center of the door. It appears that the door started bending about 400 microseconds from detonation, then reached a first peak at about 800 microseconds with a another peak following at about 1.2 milliseconds. The initial clamp strain was slightly lagging the door strain but seemed to peak at about the same time.

Figure 13 shows the strain results from gage 6H (Table 2) mounted on the inner surface of the clamp. There are two frequencies present, one at about 300Hz, relatable to the resonant motion along the length of each half-clamp section, and one at about 2kHz relatable to the flexing of clamp surfaces against door and vessel flanges.

Copyright © 2019 by ASME

Note in Figures 12 and 13, there is electrical noise from the EBW detonator firing system that appears at the beginning of the traces – this is typical in these type of high voltage, high current firing systems, as electrical noise is always coupled to the ground plane of the measurement system. Zero-time in these plots is taken as the time the detonator was provided a firing signal. It is easy to show that any mechanical impetus on the vessel cannot occur in the first 100 microseconds from detonation, and so this initial noise spike is ignored.

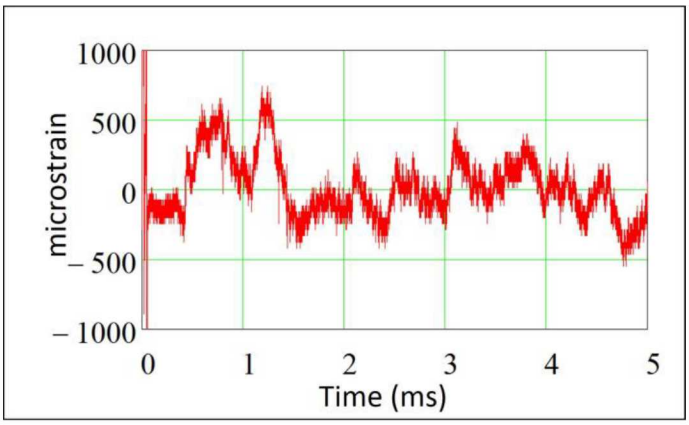

Figure 12: Door strain measured at door center (gage 7, Table 2).

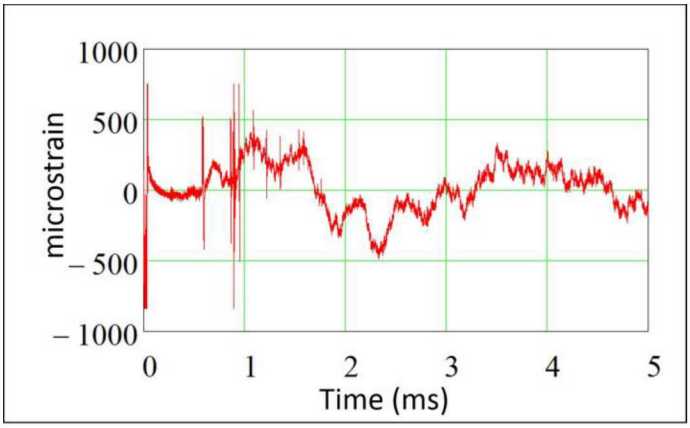

Figure 13: Inner clamp surface strain in the direction of door motion (gage 6H, Table 2).

The graph in Figure 14 shows the DIC data for displacement during the dynamic test averaged over four points near the center, four points around the edge, and one point on the electrical feedthrough flange. The inset shows the points used in the averages as white squares. The maximum dynamic displacement of the door test occurred at about 1.2ms, consistent with the strain measurements. Of note is the change in slope at about 800 microseconds – this is where the door bending was halted, but the bulk door motion continued in the outward direction. At 1.2ms, the outward door motion was halted by the clamping system, and the door returned toward the vessel. This twofold motion of the door can be better seen in Figure 14.

As with the hydrotest, the displacement was less on the left and right edges. It is interesting that the displacement returned to zero after the initial peak, but not after the second peak. The displacement after 9.5ms was about 0.4mm. There is no other evidence of a permanent displacement of the door. This offset may have resulted from a settling of the door/clamp system or from the entire vessel moving.

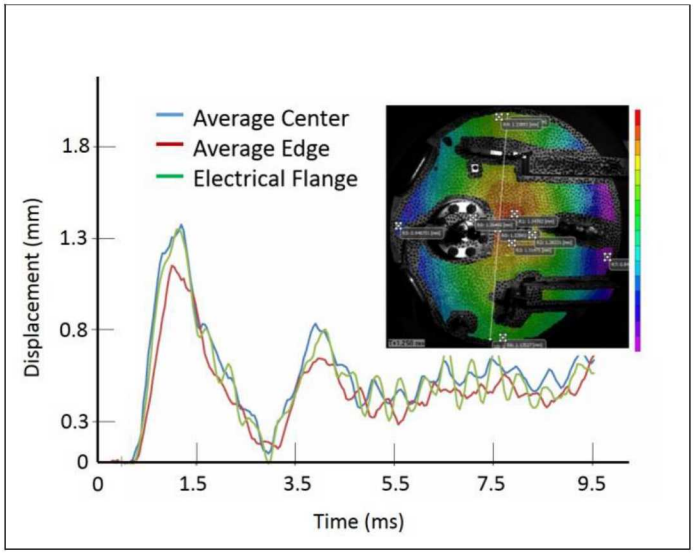

Figure 14: Dynamic displacement of door surface.

Figure 15 is an image slice across the entire surface of the door shown at several time steps. This measurement enables a review of the door movement away from the vessel, as well as any bending or deformation of the door surface. The slice location is nearly vertical and offset slightly from center line (shown in the inset of Figures 14 and 15) in order to avoid crossing of valves and door penetrations.

Analysis of this plot shows that the door starts out in bulk motion for the first 150 microseconds, starts to deflect outward to a maximum deformation of about 3 tenths of a millimeter from center to edge until about 800 microseconds, and then flattens back out at about 1ms from detonation. At about 1.2 milliseconds, the door motion is halted, and it begins its return toward the vessel body, which is consistent with the door and clamp strain data described previously. There is clearly a standing wave pattern created across the face of the door most likely due to shock reverberations across the door face and through its thickness. This effect is evident in the "wavy" nature of each trace in the figure. Perturbations from the high voltage feedthrough flange and other door penetrations are evident at the +/-300mm locations and at the door edges. This data has not been spatially filtered so as not to obscure any of these perturbations.

Copyright © 2019 by ASME

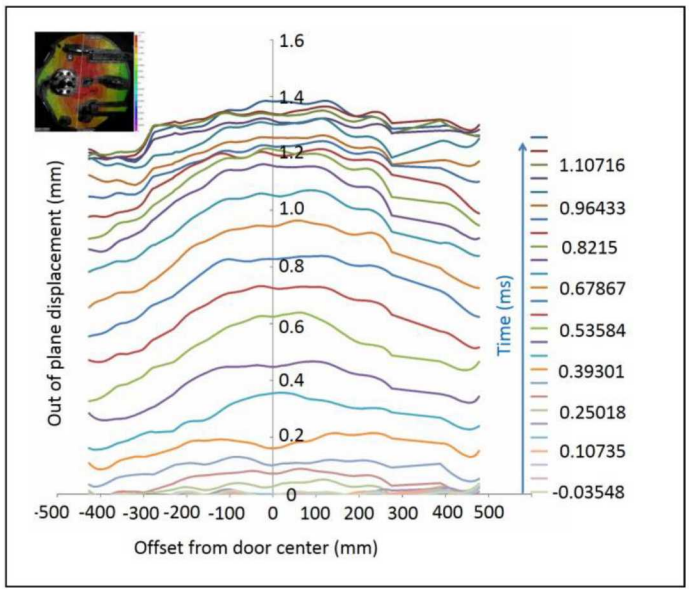

Figure 15: Temporal displacement of door surface along a slice/cut across the image.

DOOR SEAL LEAK TESTS

Helium leak rate measurements of the metal seals and valves were taken before the dynamic test. To detect transient gas leaks that might occur during the detonation, latex balloons were attached to the vacuum ports on the EDS vessel door and on the ends of some tubes. These balloons were monitored with high speed video and observed after the test to see if they were inflated. A helium leak test was also performed after the test: 1) in the annular space between the inner metal seal and the outer O-ring seal; 2) in a volume around the high voltage feedthrough flange; 3) around each valve and gage; 4) in each of the balloons.

There was a notable degradation of the leak rate of the main vessel seal after detonation and a lesser degradation in the seal around the high voltage feedthrough flange. The helium leak rates at the door seal before and after detonation were 5.2 x 10^{-8} ml-atm/sec and 3.0 x 10^{-6} ml-atm/sec respectively, a reduction of about two orders of magnitude. The helium leak rates at the high voltage flange seal before and after detonation were 7.5 x 10^{-8} ml-atm/sec and 2.1 x 10^{-7} ml-atm/sec respectively, or about one order of magnitude. Leak rates after the detonation for both seals were still well within the threshold value of 1.0 x 10^{-3} ml-atm/sec defined by the intended purpose of the system. There was no detectable helium measured around any auxiliary penetration or inside either balloon.

For this test, balloons were fitted to the leak check ports and valve outlets to capture escaping (burped) gas during the detonation (see Figures 16 and 17). After detonation the balloons had no odor of the detonation products, which were particularly pungent. Helium testing of the balloon contents (with the wand) did not detect helium. However, the annular space between the main metal seal and the secondary O-ring seal showed a transient, higher concentration before settling to a steady value. It is unclear as to the mechanism for burping. However, it is clear that none of the vessel main-body contents exited the vessel during dynamic testing. It is likely that the outer O-ring seal was breached to the exterior of the vessel, as it is designed to compress about one millimeter against the vessel door. DIC measurements indicate that the door actually moved out about 1.5mm from its original position. Therefore, we assume the balloon contents were actually exterior air entrained into the annular space between the metal seal and the O-ring, and not a breach of the metal seal to the vessel volume itself.

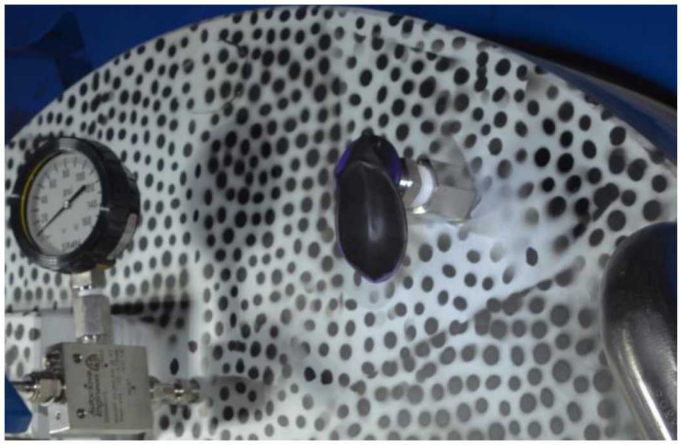

Figure 16: Pre-detonation high speed video frame of initial state of balloon.

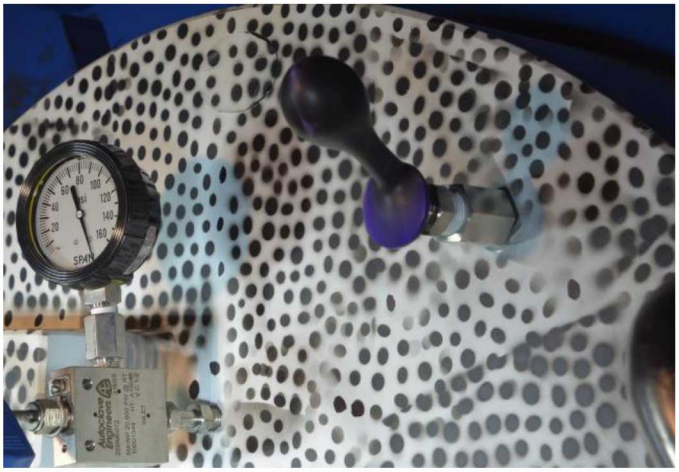

Figure 17: Post-detonation high speed video frame of balloon.

CLAMP ANALYSIS

Coupled hydrocode and finite element code analysis has been started on the clamp and seal dynamic, but it has not been completed at the time of this report. Geometric analysis of the flexing of the metal seal rings indicates that the metal seal will maintain intimate contact with the door and vessel beveled surface up to about 2.5 millimeters. Further testing will be conducted to validate this analysis.

Copyright © 2019 by ASME

CONCLUSION

It is clear from these experiments that the seal on the door under static and dynamic loading is robust. From the DIC and feeler gage results of the hydrostatic test, there appears to be a separation of the door of about 1mm from the vessel body under full static load. However, there is no loss in the vessel seal over this range. The results from the dynamic test indicates that there is a slight loss in outer O-ring seal integrity during detonation of vessel qualification loads. However, the inner, metal seal never loses contact with seal surfaces. While the sealing efficiency of the main seal experiences some degradation in performance throughout the entire process, the final leak rate of the vessel system is well within the limits prescribed by the purpose of this vessel. It is also clear that during the dynamic test, a "burp" is indeed observed, but only of the outer O-ring seal, which is meant simply to serve the purpose of providing an annular space for static helium leak measurements. Therefore, the design of the system precludes any loss of contents of the vessel beyond the primary seal. Further, this burp seems to be comprised of external air being entrained into this annular space as the door is propelled away from the vessel and returns home, rather than true vessel content or detonation products. Further testing on new vessels will bear out these suppositions.

The measurement of door strain is consistent with the measurements provided with DIC analysis of the door. Future testing will employ both strain measurements, and, either DIC measurements, or some other method for monitoring door displacement and door flexure throughout the movement of the door to ensure no loss of vessel seal during detonation of qualification explosive loads.

Lastly, it is apparent from the disparity in measurement of the vessel/door gap between the feeler gage and the DIC measurement that the vessel and door flanges which are engaged by the clamping system elastically flex during dynamic loading. Post inspection of these flanges indicated no permanent bending.

ACKNOWLEDGMENTS

This work was funded and directed by the US Army Chemical Materials Agency (CMA) Recovered Chemical Materiel Directorate (RCMD).

Sandia National Laboratories is a multi-mission laboratory managed and operated by National Technology & Engineering Solutions of Sandia, LLC, a wholly owned subsidiary of Honeywell International Inc., for the U.S. Department of Energy's National Nuclear Security Administration under contract DE-NA0003525.

This paper describes objective technical results and analysis. Any subjective views or opinions that might be expressed in the paper do not necessarily represent the views of the U.S. Department of Energy or the United States Government.

The authors would like to acknowledge the hard work, creativity and expertise of the following individuals in the completion of this work: William Adams, John Marks, US Army, Recovered Chemical Munitions Directorate; Tom Raber, Brent Haroldsen, Sandia National Laboratories, Livermore CA; Gilbert Gonzalez, Peter Montoya, Venner Saul, Megan Tribble, Sandia National Laboratories, Albuquerque, NM.

REFERENCES

[1] Haroldsen, B., Yip, M., Stofleth, J., and Caplan, A., 2013, "Experience with Using Code Case 2564 To Design and Certify An Impulsively Loaded Vessel", PVP2013-97987, Proc. of the ASME 2013 Pressure Vessels and Piping Conference, Paris, France, 7 pages.

[2] Robert Crocker, Brent Haroldsen, Jerome Stofleth, Mien Yip, "EDS Containment Vessel TNT Equivalence Testing", PVP2017-65391, Proc. of the ASME 2017 Pressure Vessels and Piping Conference, Wikaloa, HA, 7 pages.

[3] Robert Crocker, Brent Haroldsen, Jerome Stofleth, "EDS Containment Vessel Explosive Test and Analysis", PVP2016-63832, Proc. of the ASME 2016 Pressure Vessels and Piping Conference, Vancouver, BC, 8 pages.

[4] Phillip Reu, "Digital Image Correlation Best Practices", Wiley Online Library, **https://doi.org/10.1111/j.1747-1567.2011.00798.x**, January, 2012.

[5] Phillip Reu, Internal Memo, Sandia National Laboratories, July 2013.

[6] Correlated Solutions Home, **http://www.correlatedsolutions.com**

Copyright © 2019 by ASME